High-Sensitivity Detection of Carbohydrate Antigen 15-3 Using a Gold/Zinc Oxide Thin Film Surface Plasmon Resonance-Based Biosensor

ARTICLE *in* ANALYTICAL CHEMISTRY · FEBRUARY 2010

Impact Factor: 5.64 · DOI: 10.1021/ac901797j · Source: PubMed

6 AUTHORS, INCLUDING:

Chia-Chen Chang
National Taiwan University
19 PUBLICATIONS **241** CITATIONS
SEE PROFILE

Chii-Wann Lin
National Taiwan University
235 PUBLICATIONS **1,863** CITATIONS
SEE PROFILE

Anal. Chem. **2010,** *82,* 1207–1212

High-Sensitivity Detection of Carbohydrate Antigen 15-3 Using a Gold/Zinc Oxide Thin Film Surface Plasmon Resonance-Based Biosensor

Chia-Chen Chang,[†] Nan-Fu Chiu,[†] David Shenhsiung Lin,[‡] Yu Chu-Su,[†,§] Yang-Hung Liang, and Chii-Wann Lin*[,†]

Institute of Biomedical Engineering, National Taiwan University, Taipei 10617, Taiwan, Department of Medicine, National Yang-Ming University, Taipei 11221, Taiwan, and Department of Laboratory Medicine, National Taiwan University Hospital, Taipei 10002, Taiwan

We report that gold/zinc oxide (Au/ZnO) nanocomposite films were effectively employed to enhance the performance of surface plasmon resonance (SPR) for the detection of tumor markers. Carbohydrate antigen 15.3 (CA15-3), a tumor marker for breast cancer, was chosen as a model analyte. We analyzed intensity response to the samples at various concentrations (0.0125 U/mL to 160 U/mL) in pleural fluid to evaluate the detection capability of the SPR biosensor based on Au/ZnO thin films. The linear range extended from 1 to 40 U/mL with a correlation coefficient of $R^2 = 0.991$ and a limit of detection reaching 0.025 U/mL at a signal-to-noise ratio of 3:1. Compared with the degree of the shift in SPR intensity induced by the specific binding event between antibody and antigen, the change of intensity on the Au/ZnO layers was increased by at least 2 fold over that on the gold/chromium (Au/Cr) layers. In addition, we determined that the Au/ZnO layers allowed for a detection limit 4 times lower than the Au/Cr layers, which are in widespread use as the sensing interfaces in current SPR-based detectors. In conclusion, the use of Au/ZnO films greatly enhanced the SPR signal yield for this bimolecular interaction and showed high sensitivity.

In a wide variety of biosensors, it is crucial to measure the concentrations of specific biomolecules in biological fluids. Numerous investigations in recent years have focused on improving the sensitivity of biomolecular interaction detection for targets such as tumor markers,[1] viruses,[2] and bacteria.[3] Many detection assays rely on detecting the biomolecular recognition with fluorescence, radioisotope, and other types of labeling methods. However, they have several drawbacks such as low selectivity and conformational changes.[4,5] As a result, a simple, quantitative, and label-free assay is needed for molecular measurements in biomedical applications. Recently, an optical detection method utilizing the surface plasmon resonance (SPR) response was introduced.[6,7] SPR is advantageous in comparison to labeling techniques because it can detect biomolecules directly and does not require any sample probing. SPR-based biosensors have been widely applied for analyses in food,[8,9] environmental,[10,11] and biomedical science.[12−14] In addition, much research on SPR has been devoted to the development of high-throughput approaches for biomedical analysis[15−17] and the miniaturization of devices for portable analyzers.[18−20]It is a powerful optical technique offering rapid, sensitive, and high-specificity binding for the detection of target species.

For the sensor chip, a gold film has been widely utilized as a sensing substrate due to its good performance for excitation of the SPR response. Moreover, it can be simply functionalized using thiol groups in self-assembled monolayers and is easily deposited

* To whom correspondence should be addressed. E-mail: cwlinx@ntu.edu.tw. Phone: +886-2-33665271. Fax: +886-2-23620586.

† National Taiwan University.

‡ National Yang-Ming University.

§ National Taiwan University Hospital.

(1) Carrara, S.; Bhalla, V.; Stagni, C.; Benini, L.; Ferretti, A.; Valle, F.; Gallotta, A.; Ricc, B.; Samor, B. *Sens. Actuators, B* **2009**, *136*, 163–172.

(2) Lee, S. Y.; Lee, C. N.; Mark, H.; Meldrum, D. R.; Lin, C. W. *Sens. Actuators, B* **2007**, *127*, 598–605.

(3) Shriver-Lake, L. C.; Turner, S.; Taitt, C. R. *Anal. Chim. Acta* **2007**, *584*, 66–71.

(4) Ramachandran, R.; Larson, D. N.; Stark, P. R. H.; Hainsworth, E.; LaBaer, J. *FEBS J.* **2005**, *272*, 5412–5425.

(5) Ramanavicius, A.; Kurilcik, N.; Jursenas, S.; Finkelsteinas, A.; Ramanaviciene, A. *Biosens. Bioelectron.* **2007**, *23*, 499–505.

(6) Homola, J. *Anal. Bioanal. Chem.* **2003**, *377*, 528–539.

(7) Boozer, C.; Kim, G.; Cong, S.; Guan, H.; Londergan, T. *Curr. Opin. Biotechnol.* **2006**, *17*, 400–405.

(8) Nanduri, V.; Bhunia, A. K.; Tu, S.-I.; Paoli, G. C.; Brewster, J. D. *Biosens. Bioelectron.* **2007**, *23*, 248–252.

(9) Spadavecchia, J.; Manera, M. G.; Quaranta, F.; Siciliano, P.; Rella, R. *Biosens. Bioelectron.* **2005**, *21*, 894–900.

(10) Mauriz, E.; Calle, A.; Manclús, J.; Montoya, A.; Lechuga, L. *Anal. Bioanal. Chem.* **2007**, *387*, 1449–1458.

(11) Mauriz, E.; Calle, A.; Montoya, A.; Lechuga, L. M. *Talanta* **2006**, *69*, 359–364.

(12) Carrascosa, L.; Calle, A.; Lechuga, L. *Anal. Bioanal. Chem.* **2009**, *393*, 1173–1182.

(13) Foley, K. J.; Forzani, E. S.; Joshi, L.; Tao, N. *Analyst* **2008**, *133*, 744–746.

(14) Murphy, A. J.; Kemp, F.; Love, J. *Anal. Biochem.* **2008**, *376*, 61–72.

(15) Nedelkov, D. *Anal. Chem.* **2007**, *79*, 5987–5990.

(16) Shumaker-Parry, J. S.; Aebersold, R.; Campbell, C. T. *Anal. Chem.* **2004**, *76*, 2071–2082.

(17) Takeda, H.; Fukumoto, A.; Miura, A.; Goshima, N.; Nomura, N. *Anal. Biochem.* **2006**, *357*, 262–271.

(18) Huang, J. G.; Lee, C. L.; Lin, H. M.; Chuang, T. L.; Wang, W. S.; Juang, R. H.; Wang, C. H.; Lee, C. K.; Lin, S. M.; Lin, C. W. *Biosens. Bioelectron.* **2006**, *22*, 519–525.

(19) Stevens, R. C.; Soelberg, S. D.; Near, S.; Furlong, C. E. *Anal. Chem.* **2008**, *80*, 6747–6751.

(20) Suzuki, M.; Ozawa, F.; Sugimoto, W.; Aso, S. *Anal. Bioanal. Chem.* **2002**, *372*, 301–304.

10.1021/ac901797j
Published on Web 01/26/2010

by a thermal evaporation process. In most chip configurations, glass serves as the supporting substrate, but it does not adhere strongly to gold materials. Cr is the most frequently used metal nanomaterial to improve the adherence of gold films to glass substrates. However, it has several problems involving metal interdiffusion and low optical transmission to the gold surface.[21,22] These events result in a change in the gold's surface properties and may affect the sensitivity and stability of optical experiments. Therefore, the development of more ideal nanomaterials may be the innovation required in biosensor substrates to increase the detection sensitivity. As a nanomaterial, ZnO nanostructures exhibit excellent optical and electrical properties such as a wide band gap, high transparency, and low resistivity.[23,24] Recently, many studies have been carried out exploring Au/ZnO nanocomposites because of their desirable optical properties.[25−27] Nevertheless, the applications of Au/ZnO nanoscale thin films in biosensors have not yet been comprehensively realized.

The detection and quantitation of a tumor marker in a bodily fluid sample of a patient can provide meaningful information involving the progression of many cancers. For example, carbohydrate antigen 15.3 (CA15-3), encoded by the gene MUC1, has been considered for clinical use in breast carcinoma diagnosis for at-risk women,[28] where a CA15-3 level of 30 U/mL is considered a threshold value. In addition to breast cancer, CA15-3 is overexpressed in several other malignant conditions such as ovarian, colon, lung, and pancreatic cancer.[29−33] Although CA15-3 concentration is elevated in only 10% of patients with stage I breast cancer, and so it is not used for the purposes of early diagnosis,[34] it is still considered an important prognosis factor due to the high preoperative concentrations of CA15-3 seen in up to 80% of metastatic breast cancers.[35] The first CA 15-3 assay was developed for use in radioisotopic detection.[36] This protocol included complicated steps and hazardous radioisotopes, leading to a slow process and a dangerous detection environment. Consequently, radioisotopic immunoassay has been gradually replaced by non-radiochemical techniques such as enzyme immunoassay[37] and chemiluminescence immunoassay.[38] Although these conventional assays are quite reliable, they are also time- and labor-consuming methods. In contrast, optical biosensors with high-resolution, label-free, and real-time analysis could overcome these problems. Therefore, CA15-3 was investigated as an analytical model with a novel thin film-based SPR device.

In this study, we present an immunosensing application of a novel Au/ZnO-based biosensor for the detection of a tumor marker. The sensitivity of CA15-3 detection in diluted pleural fluid samples was determined by an Au/ZnO thin film SPR and compared with that of a conventional Au/Cr-based SPR biosensor. Surface roughness and specificity of the sensor systems were also evaluated. The results show that an Au/ZnO SPR offers a potentially powerful assay, with a highly sensitive analysis, that may be applicable as an important tool for tumor marker detection.

MATERIALS AND METHODS

Materials. All chemical reagents used were of analytical grade. 1-Ethyl-3-(3-dimethylaminopropyl)carbodiimide hydrochloride (EDC), *N*-hydroxysuccinimide (NHS), and bovine serum albumin (BSA) were purchased from Sigma. 10× Phosphate-buffered saline (PBS) solution, pH 7.4, was purchased from Gibco-Invitrogen. 8-Mercaptooctanoic acid ($C_8H_{16}O_2S$; 8-MOA) was provided by Prof. Adam Shih-Yuan Lee from the Department of Chemistry at Tamkang University and was dissolved in absolute ethanol, which was purchased from ECHO Chemical. Monoclonal antibody against the human breast carcinoma-associated antigen was purchased from Abcom.

The sample of human tumor marker, CA15-3, was collected from the pleural fluid of a breast cancer patient and was provided by the Department of Laboratory Medicine at National Taiwan University Hospital. An aliquot of pleural fluid was measured, and the remaining pleural fluid was stored at −20 °C. The quantitative determinations of CA15-3 in pleural fluid were made using a standard kit in an Abbott Architect i2000 immunoassay analyzer. Standard samples without impurities were purchased from Abbott Laboratories.

Fabrication of Chip Substrates. Two different sensing substrates, the Au/Cr layers and the Au/ZnO layers, were used for the experiments. Standard glass microscope slides (SF-10, Schott Glass) were used as base substrates. To remove any contaminants, the glass substrates were subjected to ultrasonic cleaning in piranha solution (H_2SO_4:H_2O_2 = 3:1) for 10 min and then rinsed three times with deionized water in an ultrasonic bath before deposition. The slides were finally dried with nitrogen gas.

Both of the thin films grown on the glass substrates are shown in Figure 1. Cr and Au films were deposited by an electron beam evaporator at a vacuum level of about 3×10^{-6} Torr. The ZnO film was grown on a glass substrate using a radiofrequency (RF; 13.56 MHz) sputtering system. A working pressure of 3 mTorr was employed during the deposition, and a mixture of Ar (40%) and O_2 (30%) was used as the working gas.

(21) Holloway, P. H. *Gold Bull.* **1979**, *12*, 99.
(22) Neff, H.; Zong, W.; Lima, A. M. N.; Borre, M.; Holzhuter, G. *Thin Solid Films* **2006**, *496*, 688–697.
(23) Ozgur, U.; Alivov, Y. I.; Liu, C.; Teke, A.; Reshchikov, M. A.; Dogan, S.; Avrutin, V.; Cho, S. J.; Morkoc, H. *J. Appl. Phys.* **2005**, *98*, 041301−041103.
(24) Djurišić, A. B.; Leung, Y. H. *Small* **2006**, *2*, 944–961.
(25) Liao, H. *Opt. Lett.* **2003**, *28*, 1790.
(26) Wang, X.; Kong, X.; Yu, Y.; Zhang, H. *J. Phys. Chem. C* **2007**, *111*, 3836–3841.
(27) Mosbacker, H. L.; Strzhemechny, Y. M.; White, B. D.; Smith, P. E.; Look, D. C.; Reynolds, D. C.; Litton, C. W.; Brillson, L. J. *Appl. Phys. Lett.* **2005**, *87*, 012102−012103.
(28) Uehara, M.; Kinoshita, T.; Hojo, T.; Akashi-Tanaka, S.; Iwamoto, E.; Fukutomi, T. *Int. J. Clin. Oncol* **2008**, *13*, 447–451.
(29) von Mensdorff-Pouilly, S.; Snijdewint, F. G.; Verstraeten, A. A.; Verheijen, R. H.; Kenemans, P. *Int. J. Biol. Markers* **2000**, *15*, 343–356.
(30) Richards, E. R.; Devine, P. L.; Quin, R. J.; Darrell Fontenot, J.; Ward, B. G.; McGuckin, M. A. *Cancer Immunol. Immunother.* **1998**, *46*, 245–252.
(31) Nakamura, H.; Hinoda, Y.; Nakagawa, N.; Makiguchi, Y.; Itoh, F.; Endo, T.; Imai, K. *J. Gastroenterol.* **1998**, *33*, 354–361.
(32) Kotera, Y.; Fontenot, J. D.; Pecher, G.; Metzgar, R. S.; Finn, O. J. *Cancer Res.* **1994**, *54*, 2856–2860.
(33) Dupont, J.; Tanwar, M. K.; Thaler, H. T.; Fleisher, M.; Kauff, N.; Hensley, M. L.; Sabbatini, P.; Anderson, S.; Aghajanian, C.; Holland, E. C.; Spriggs, D. R. *J. Clin. Oncol.* **2004**, *22*, 3330–3339.
(34) Duffy, M. J. *Clin. Chem.* **2006**, *52*, 345–351.
(35) De La Lande, B.; Hacene, K.; Floiras, J. L.; Alatrakchi, N.; Pichon, M. F. *Int. J. Biol. Markers* **2002**, *17*, 231–238.
(36) Tobias, R.; Rothwell, C.; Wagner, J.; Green, A.; Liu, Y. S. W. *Clin. Chem.* **1985**, *31*, 986.
(37) Muller, V.; Stahmann, N.; Riethdorf, S.; Rau, T.; Zabel, T.; Goetz, A.; Janicke, F.; Pantel, K. *Clin. Cancer Res.* **2005**, *11*, 3678–3685.
(38) Bon, G. G.; von Mensdorff-Pouilly, S.; Kenemans, P.; van Kamp, G. J.; Verstraeten, R. A.; Hilgers, J.; Meijer, S.; Vermorken, J. B. *Clin. Chem.* **1997**, *43*, 585–593.

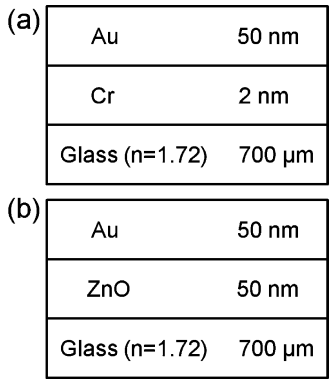

Figure 1. Schematic diagram of the thin film structure (not drawn to scale) in (A) Au/Cr and (B) Au/ZnO. The refractive indices of a ZnO film and a Cr film are 1.98 and 4.14, respectively.

Analysis of Bare Gold Surfaces. The bare gold surface roughness was measured by atomic force microscopy (AFM) (NanoInk, Chicago, IL) in air at room temperature. AFM imaging was done in contact mode on selected areas of $5 \times 5\ \mu m^2$ on the samples. Data acquisition and analysis were performed using InkCAD software (NanoInk, Chicago, IL). The scan rate was 2.0 Hz.

Optical Property Measurements. The transmission spectra were recorded using a Cary 50 UV−vis spectrophotometer (Varian Inc., Palo Alto, CA) with wavelength in range of 400−900 nm. Optical properties of SPR reflectivity curves were carried out with an imaging ellipsometer (Nanofilm Inc., Göttingen, Germany), at an incident angle of 43° and a wavelength of 833 nm.

Surface Functionalization of the Gold Surface. Prior to surface functionalization, the gold-coated glass slide was washed with a detergent and the ethanol solution and then rinsed with Milli-Q water with sonication. The assay developed was designed as a bioaffinity immobilization assay. The gold-coated slide was immersed into an 8-MOA solution at room temperature for 20 min to form a self-assembled monolayer on the surface. Then, the chemically immobilized surface was activated using 400 mM EDC/100 mM NHS for covalent bond formation for 10 min at room temperature. The gold film chip was then soaked in a 50 μg/mL protein G solution and allowed to fix onto the gold surface for 10 min. The antibody, at a concentration of 5 μg/mL, was then immobilized onto the surface for 20 min and the surface was blocked with 1% BSA for 10 min.

SPR-Based Bioassay for CA15-3 Detection. Binding reactions were analyzed using SPRimager instrumentation (GWC Technologies, Madison, WI), where changes in SPR were monitored in real time as the analyte was passed over the sensor chip. Measurements were based on the setup of a prism coupled SPR, first introduced by Kretschmann.[6] The measured response values are expressed in arbitrary units (a.u.). A patient sample with a known concentration of the breast cancer marker CA15-3 was diluted with PBS to obtain various concentrations from 0.0125 to 160 U/mL. To minimize mass transport effects, a high flow rate (40 μL/min) was employed.[39] The Au/Cr and Au/ZnO chips were prepared to measure the intensities of reflected light at the respective angles of 50.5° and of 51° at 790 nm wavelength. In the initial step, the gold surface was exposed to PBS buffer in order to obtain a stable baseline. Then, CA15-3 in PBS at different concentrations was injected onto the immobilized surface. PBS was finally allowed to flow through the immobilized surface to wash away unbound molecules.

(39) Myszka, D. G. *Curr. Opin. Biotechnol.* **1997**, *8*, 50–57.

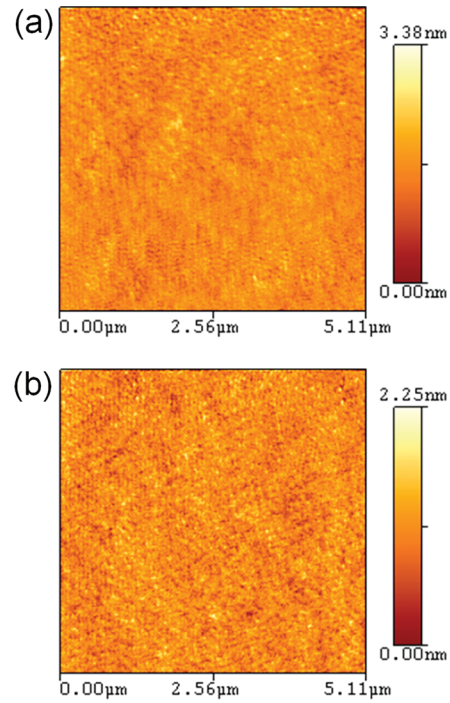

Figure 2. Contact mode AFM images of (a) the bare Au/Cr films and (b) the bare Au/ZnO films in top-view representations.

Data Analysis. All experiments were run in triplicate. Calibration curves were calculated using Sigma Plot software and analyzed with a four-parameter logistic equation as follows,[40]

$$Y = B + \frac{(A - B)}{1 + \left(\frac{X}{C}\right)^D}$$

where Y is the SPR intensity signal, X is the analyte concentration, A is the highest relative intensity of SPR detection, B is the lowest relative intensity of SPR detection, C is the concentration that exhibits the half maximal relative intensity, and D is the slope at the inflection point of the calibration curve.

RESULTS AND DISCUSSION

Characterization of Sensor Surfaces. The performances of SPR biosensors depend not only on the optical properties of the optical components but also on the morphological details of the different interfaces, especially for the free surface. Therefore, it is necessary to have an excellent characterization of the morphology to exclude this contribution as a dominant effect in the SPR response. To investigate the surface morphology, AFM was used for the topographic characterization of the Au/Cr and Au/ZnO nanocomposite films. Figure 2 shows top-view images of the bare gold slide. The rms (root-mean-square) roughnesses for the Au/Cr and the Au/ZnO bare gold surfaces were 0.27 and 0.26 nm, respectively. Deposition of gold films onto the ZnO surface did

(40) O'Connell, M. A.; Belanger, B. A.; Haaland, P. D. *Chemometrics Intell. Lab. Syst.* **1993**, *20*, 97–114.

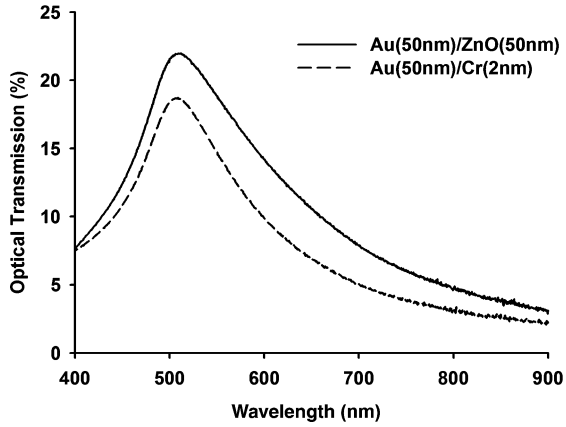

Figure 3. The measured transmission spectrum of the Au/Cr layer (dash line) and the Au/ZnO layer (solid line).

not induce any topographic changes on the sensor surface. The topographies both exhibited a lack of large features and similar roughnesses, with regular nanopits. Moreover, the variations of roughness were within the 0.2 nm scale. In a previous study, the SPR response did not have a significant influence on detection when the roughness of the gold surface was smaller than 1 nm.[41] Thus, the possibility of unstable SPR signal due to the roughness of the bare gold was eliminated and the main effect of SPR response on the surface roughness can be excluded.

Optical Transmittance. The UV−vis transmission spectra of the different adhesion substrates with a 50 nm gold film, covering a range of wavelengths between 400 and 900 nm, are shown in Figure 3. The response measured through an Au/Cr film exhibits a transmission peak near 500 nm, which is consistent with the green region of the spectrum in the transparent gold film. An Au/ZnO thin film also shows a similar response curve. However, the Au layer with Cr thickness of 2 nm has a lower transparency compared to Au/ZnO thin layer due to light absorption in the Cr thin film.

SPR Reflectivity Curves for the Au/Cr Layer and the Au/ZnO Layer. For the better performance of a SPR biosensor, the narrower resonance in the SPR curve is desired.[42] Thus, the influence of the intermediate thin films was evaluated with $\Delta\theta$ and fwhm (full width at half-maximum of the resonance dip). Figure 4 showed the resulting SPR curves when the Au/Cr and the Au/ZnO layers were in contact with molecules in the immobilization procedure. As a result, an Au/ZnO layer showed a greater increase in the resonance angle and a narrower fwhm in the reflectivity curve. In contrast, a conventional film gave rise to a weaker angle shift and a wider fwhm in the SPR spectrum and curve, respectively (Table 1). Accordingly, the major factor influencing the performance in the SPR spectrum was a change in the fwhm of the Au/ZnO nanocomposite film.

Detection of CA15-3 by the Au/ZnO Thin Film SPR. To achieve a high sensitivity and specificity in immunoassays, it is critical for the antibody immobilization process to result in their correct orientation on the sensor surface so that the analytes can access the antibody active sites and thus be bound. Antibodies

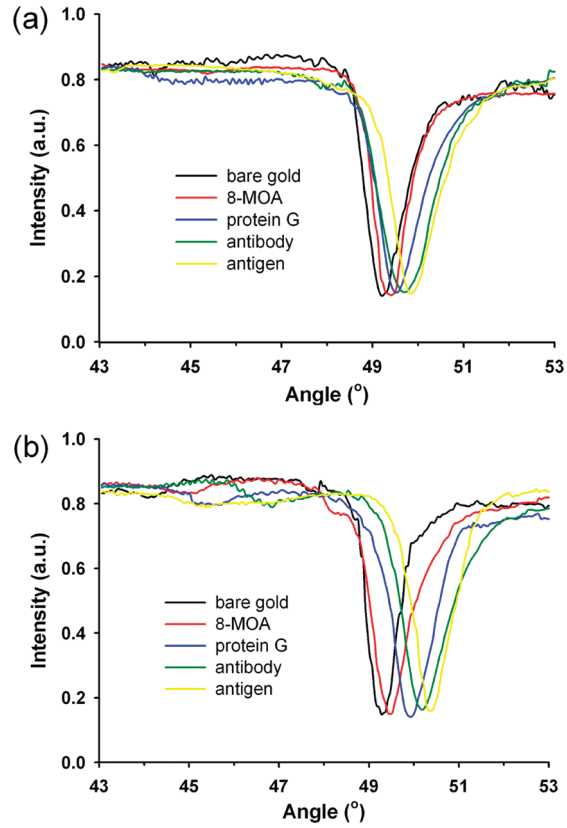

Figure 4. Normalized SPR reflectivity curves for the (a) the Au/Cr interfaces and (b) the Au/ZnO interfaces when immobilizing the molecules onto the interfaces: Bare gold (black); 10 mM 8-MOA SAM (red); 50 μg/mL protein G (blue); 5 μg/mL CA15-3 antibody (green); 40 U/mL CA15-3 antigen (yellow).

Table 1. Comparison of Measured Angle Shifts and FWHM between the Au/Cr and Au/ZnO SPR Thin Films

	$\Delta\theta$ SPR (deg)		fwhm (deg)	
	Au/Cr	Au/Zno	Au/Cr	Au/Zno
bare gold	0	0	1.10	0.85
8-MOA	0.19	0.20	1.01	0.95
protein G	0.15	0.40	1.20	1.10
antibody	0.14	0.29	1.39	1.25
antigen	0.10	0.20	1.24	1.05

immobilized in a highly oriented manner maintain higher binding capacity than those in a random manner.[43] Protein G, a surface protein from a streptococcal strain, can lead to immune escape because it is generally expected to bind to the Fc part of the antibody specifically. This provides specific affinity binding sites for interaction with antibodies.[44] The possibility of any functional damage to the antibodies due to random coupling is also eliminated. Hence, in this study, bioaffinity immobilization using protein G was adopted for the assay.

Interaction of the antigen with the antibody layer was determined by monitoring relative intensity changes on the sensing surface and followed by recording the phase of the intensity in

(41) Byun, K. M.; Yoon, S. J.; Kim, D.; Kim, S. J. *J. Opt. Soc. Am. A* **2007**, *24*, 522–529.
(42) Sherry, L. J.; Chang, S. H.; Schatz, G. C.; Duyne, R. P. V. *Nano Lett.* **2005**, *5*, 2034–2038.
(43) Babacan, S.; Pivarnik, P.; Letcher, S.; Rand, A. G. *Biosens. Bioelectron.* **2000**, *15*, 615–621.
(44) Muñoz, E.; Vidarte, L.; Pastor, C.; Casado, M.; Vivanco, F. *Eur. J. Immunol.* **1998**, *28*, 2591–2597.
(45) Zhang, H. G.; Qi, C.; Wang, Z. H.; Jin, G.; Xiu, R. J. *Clin. Chem.* **2005**, *51*, 1038–1040.

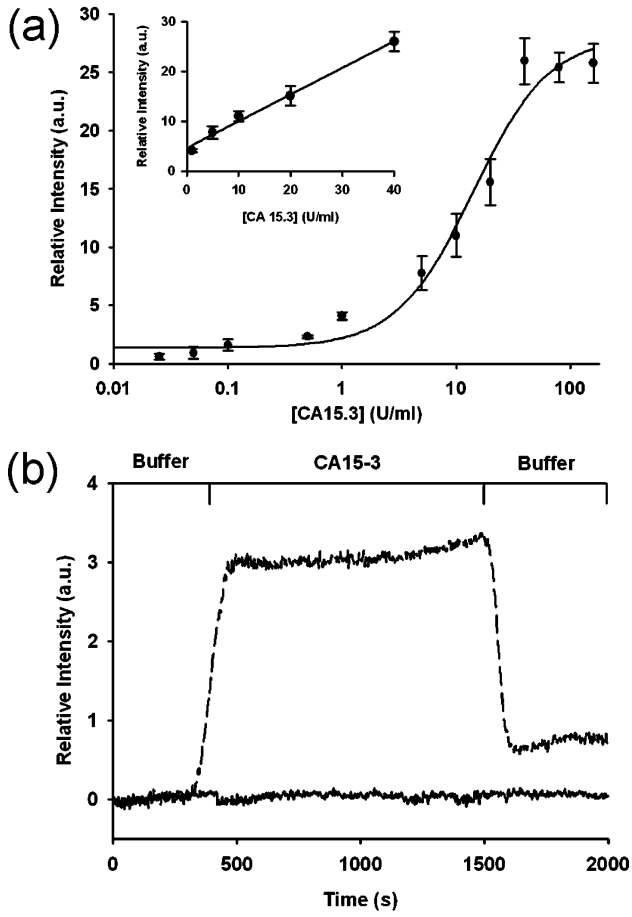

Figure 5. (a) Calibration curve for the determination of CA15-3 (with solutions containing 0.025, 0.05, 0.1, 0.5, 1, 5, 10, 20, 40, 80, and 160 U/mL) with an Au/ZnO-based biosensor. Inset shows the response of the SPR biosensor from 1 U/mL to 40 U/mL with a correlation coefficient (R^2) of 0.991. (b) Real-time intensity of CA15-3 antigen as detected by the Au/ZnO thin film biosensor. The dashed line represents the detection of CA15-3 antigen (0.025 U/mL). The solid line is the negative control.

real time. A calibration curve, shown in Figure 5a, was obtained from triplicate measurements of CA15-3 concentrations ranging from 0.0125 U/mL to 160 U/mL. The experimental data gave good agreement when fitted to the calibration curve, with a correlation coefficient (R^2) of 0.979. It was obvious that the SPR intensity response increased with an increase in the CA15-3 antigen concentration but only up to a point; when the concentration of antigen was over 40 U/mL, the intensity response reached saturation. The linear range for the determination of CA15-3 was from 1 U/mL to 40 U/mL, exhibiting a good linearity with a correlation coefficient (R^2) of 0.991 (inset in Figure 5a). Thus, when CA15-3 concentrations over 40 U/mL resulted in higher signal responses, it could not be quantified reliably. The more concentrated samples needed to be diluted to within the linear range of the biosensor.

Figure 5b shows the SPR responses to the binding of 0.025 U/mL CA15-3 from the patient sample to the antibody-functionalized sensor surface. For detection of CA15-3, sample concentrations of 0.025 U/mL and above resulted in significant intensity changes. The SPR intensity of the control had an average value of 0.02 ± 0.13 au. To establish the limit of detection (LOD), it was defined as three times the standard deviation of the control.

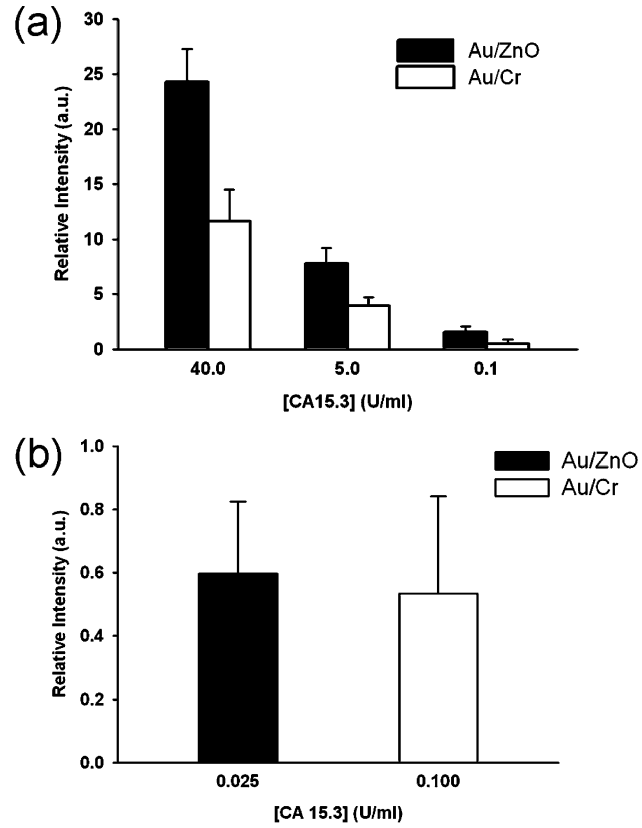

Figure 6. Averages of SPR intensity measured for the adsorption of antigen to antibody (a) at different concentrations and (b) at the detection limit of concentration on the Au/ZnO layers and the Au/Cr layers. Error bars indicate the standard deviation for the mean of three measurements.

Hence, the LOD was determined to be 0.025 U/mL because this level resulted in an average value of 0.60 ± 0.23 au.

Comparative Analysis of CA15-3 Detection by Au/Cr and Au/ZnO Thin Film SPR. The intensity changes of two different thin film SPR devices induced by adsorbing CA15-3 at different concentrations (40, 5, and 0.1 U/mL) are shown in Figure 6a. The phase of the intensity on the Au/ZnO-based sensor was increased by 2-fold over that on the Au/Cr layers in 40 U/mL as well as in 5 U/mL. However, with the lower concentrations, such as 0.1 U/mL, the Au/ZnO-based biosensor could improve the sensitivity of detection 3-fold compared with the conventional sensing substrate-based biosensor. Moreover, in the LOD of SPR, as shown in Figure 6b, the Au/Cr and Au/ZnO film biosensors reached 0.1 U/mL and 0.025 U/mL, respectively. In other words, the detection limit with the Au/ZnO layers was approximately 4-fold lower than that for the Au/Cr layers.

The threshold value of CA15-3 concentration in healthy individuals is 30 U/mL, indicating that the sensitivities of these two kinds of thin film-based SPR are adequate to detect this level. A conventional SPR biosensor could detect the concentration down to 0.1 U/mL, whereas a newly developed SPR biosensor is capable of sensing 0.025 U/mL CA15-3. These results demonstrated that the Au/ZnO thin film SPR could detect a weaker affinity interaction than the conventional SPR biosensor could.

The LOD of the biosensor based on the Au/ZnO thin film is comparable or superior to the detection limits for tumor marker recently reported using other biosensing techniques. The Au/

ZnO thin film SPR biosensor achieved a detection limit (0.025 U/mL) lower than any of the other biosensors (1 U/mL for the imaging ellipsometry[45] and 2.5 U/mL for the scanning electrochemical microscopy[46]). Although this assay showed a narrower linear range in the detection of CA15-3, the LOD was also better than the minimum detectable concentration obtained using electrochemical immunoassay,[47] capillary electrophoretic immunoassay,[48] and chemiluminescent immunoassay.[49] The capillary electrophoretic enzyme immunoassay with electrochemical assay (CE-EIA-ED) showed nearly the same minimum detectable concentration as the Au/ZnO thin film SPR biosensor of 0.025 U/mL.[50] Compared with CE-EIA-ED, based on an HRP-functionalized antibody label, this novel SPR had the advantage of label-free detection. As a result, the measurements by SPR could be performed faster than that with CE-EIA-ED including a 1 h incubation time. It can therefore be concluded that an Au/ZnO thin film is an ultrasensitive sensing substrate for CA15-3 measurement.

Correlation between Antibody Detection of CA15-3 Antigen in Pleural Fluid and of Antigen in Standard Solution. To investigate the clinical applicability of the newly developed thin film SPR sensor, the specificity was examined by analyzing CA15-3 standard samples with five concentrations (40, 20, 5, 1, 0.025 U/mL). Figure 7 describes the correlation results between the detections of CA15-3 in pleural fluid samples and in standard samples. The linear relation had a slope of 1.754 with a correlation coefficient (R^2) was 0.994. These results indicated that nonspecific binding and cross-reactivity in CA15-3 detections did not evidently interfere with the response of the biosensor. Consequently, it is feasible to use the newly developed thin film SPR sensor to detect CA15-3 in clinical diagnostics.

CONCLUSIONS

Herein, we provide a new analytical assay for the detection of tumor marker using an Au/ZnO thin film SPR biosensor with high sensitivity. A SPR biosensor with an intermediate thin film of ZnO showed a narrow fwhm and a large angle shift. Thus, this sensor exhibited up to a 4-fold higher response than that of the conventional Au/Cr-based SPR sensor and can detect CA15-3 directly in pleural fluid samples. Furthermore, our assay developed for the CA15-3 antigen, with an LOD of 0.025 U/mL, is more sensitive than those previously reported.[45−50] The assay described in this work is very simple, does not require complicated sample treatment procedures, and employs inexpensive reagents for analysis. Moreover, it is a label-free detection without additional amplification steps to enhance the sensitivity. Therefore, this SPR biosensor can provide a highly sensitive immunosensing system and serve as a good alternative detection technique to the conventional SPR immunosensor for tumor diagnosis.

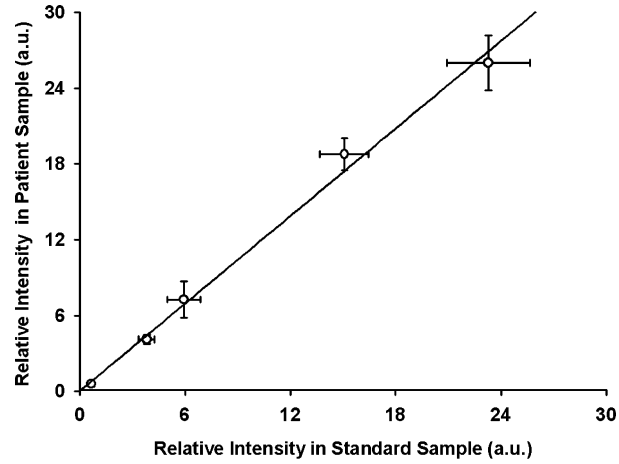

Figure 7. Correlation between the results obtained in the patient samples and the standard samples of CA 15−3 with five concentrations (40, 20, 5, 1, 0.025 U/mL) ($R^2 = 0.994$). Error bars indicate the standard deviation for the mean of three measurements.

ACKNOWLEDGMENT

This work was supported by the National Science Council of ROC under contract number NSC 95-2218-E-002-054-MY3.

Received for review August 9, 2009. Accepted January 4, 2010.

AC901797J

(46) Zhang, X.; Peng, X.; Jin, W. *Anal. Chim. Acta* **2006**, *558*, 110–114.
(47) Hong, C.; Yuan, R.; Chai, Y.; Zhuo, Y. *Anal. Chim. Acta* **2009**, *633*, 244–249.
(48) Liu, Y. M.; Zheng, Y. L.; Cao, J. T.; Chen, Y. H.; Li, F. R. *J. Sep. Sci.* **2008**, *31*, 1151–1155.
(49) Fu, Z.; Yang, Z.; Tang, J.; Liu, H.; Yan, F.; Ju, H. *Anal. Chem.* **2007**, *79*, 7376–7382.
(50) He, Z.; Gao, N.; Jin, W. *J. Chromatogr., B* **2003**, *784*, 343–350.